archives
of thermodynamics
Vol. **44**(2023), No. 2, 69–85
DOI: 10.24425/ather.2023.146559

Study of the effect of geometric shape on the quality of mixing: Examining the effect of length of the baffles

MALIKA SEDDIK BOUCHOUICHA[a]
HOUSSEM LAIDOUDI[a*]
SOUAD HASSOUNI[a]
OLUWOLE DANIEL MAKINDE[b]

[a] University of Science and Technology of Oran Mohamed-Boudiaf, Faculty of Mechanical Engineering, BP 1505, El-Menaouer, Oran, 31000, Algeria

[b] Stellenbosch University, Faculty of Military Science, Private Bag X2, Saldanha 7395, South Africa

Abstract This work is an attempt to study the behaviour of fluid in the mixing vessel with a two-bladed or four-bladed impeller. The working fluid is complex, of a shear-thinning type and the Oswald model is used to describe the fluid viscosity. The study was accomplishedby numerically solving the governing equations of momentum and continuity. These equations were solved for the following range of conditions: 50–1000 for the Reynolds number, 0–0.15 for the baffle length ratio, and the number of impeller blades 2 and 4. The simulations were done for the steady state and laminar regime. The results show that the increase in baffle length (by increasing the ratio baffle length ratio) decreases the fluid velocity in the vessel. Increasing the speed of rotation of the impeller and/or increasing the number of blades improves the mixing process. Also, the length of the baffles does not affect the consumed power.

Keywords: Baffles; Stirred vessel; Non-Newtonian fluid, Steady simulation, CFD

*Corresponding Author. Email: houssem.laidoudi@univ-usto.dz

Nomenclature

D	–	diameter of the vessel, m
H	–	height of the vessel, m
h	–	diameter of the impeller, m
k_s	–	weak function factor
l	–	length of the baffle, m
m	–	fluid consistency, Pa s^n
N	–	rotational velocity, rad/s
n	–	power-law index
N_p	–	power number
P	–	mechanical power, W
p	–	pressure, Pa
p^*	–	dimensionless pressure
Q_v	–	viscous dissipation, m/s^2
R^*	–	dimensionless diameter
r, θ, z	–	cylindrical coordinates
Re	–	Reynolds number
V_r	–	radial velocity, m/s
V_z	–	axial velocity, m/s
V_θ	–	tangential velocity, m/s

Greek symbols

$\dot{\gamma}$	–	shear rate, 1/s
μ	–	dynamic viscosity, Pa s
ρ	–	density, kg/m^3
τ	–	shear stress, Pa

1 Introduction

The study of mechanical agitation is considered one of the most important studies that witnessed the interest of many researchers recently. This is mainly due to its sensitive presence in many areas of industry including the pharmaceutical industry, food manufacturing, cosmetics manufacturing, medical analyses and so on.

The mixing process using a mechanical mixer is evaluated by two main factors, namely: the quality of the mixture obtained and the duration of mixing with the mechanical energy consumed. Therefore, the research in this field aims at designing of a mixer capable of mixing the fluid effectively with the effects of saving energy and mixing time.

There are quite a few researchers who have investigated in this direction. Hadjeb *et al.* [1] researched the shape of the agitator by combining two

previous simple shapes of an agitator, namely: a helical screw and a two-blade impeller. The fluid studied in this paper was that of a highly viscous fluid, while the vessel had a simple cylindrical type without any baffle. The results of the research showed that this new form has the ability to raise the quality of mixing. Laidoudi [2] accomplished a numerical work on the effect of shape of the mixer on the quality of mixing. The form studied in this paper consists in holes in the blades of the two-bladed agitator. The form of the vessel was cylindrical without baffles. The working fluid was Newtonian and the flow regime was perfectly laminar. The results showed that this new form has a tendency to improve the mixing quality. Ameur [3] studied the effect of the form of the vessel on the mixing quality, while the form of the impeller was kept fixed (Scaba 6SRGT- six-curved bladed impeller impeller). The forms studied here are: a dished bottomed cylindrical vessel, a flat bottomed cylindrical vessel and a closed spherical vessel. The results of the research confirm that the shape of the vessel affects the quality of mixing.

There is also a group of researchers who studied mixing of complex fluids using a mechanical agitator where the impeller has curved blades [4–12]. Some investigators [13–19] also studied the effect of baffles inside the vessel on the quality of mixing. The behaviour of the fluid in the vessel has been understood with the determination of energy consumed.

Ameur [20] conducted the numerical simulation of shear-thinning fluid in a cylindrical vessel stirred by a turbine. The study examined the effect of impeller shape on the characteristics of mixing. The mechanical power consumed by the impeller has been evaluated according to the power number. The model of Oswald has been used to define the viscosity.

There are also other works [21–32] that have studied different groups of fluids inside vessels with mechanical agitators of different shapes and sizes. Furthermore, recent studies show that the fluid motion inside the vessels is mainly related to the geometry of the vessel and rotating objects [33–44]. Generally, it can be concluded that the performance of the mixer and the mixing process can actually be improved if the process is analyzed and the effects of the engineering parts are known.

From the aforementioned previous investigations, the following becomes clear: the mixing process for complex fluids is one of the most important factors in industrial applications such as the manufacture of medicines, organic compounds and foodstuffs. Also, the mixing process is related to the geometric shape of the mixer and the quality of the fluid. In addition to this, each fluid must be studied in order to know its exact behaviour.

Accordingly, this work presents a study of a type of complex fluid inside a mixer. The general shape of the mixer undergoes geometric changes in order to determine the shape that helps in accelerating the process of mixing the fluid and reducing the mechanical energy consumed. Accordingly, the elements studied here are: the speed of rotation of the impeller, the number of blades and the length of baffles placed in the vessel.

This research can be used to enhance results related to industrial applications such as the process of mixing pharmaceuticals, cosmetics and alimentary. This research can also be a reference for pedagogical works related to the mixing process.

2 The studied system

The mixing system studied in this paper is presented in Fig. 1. The system mainly consists of a flat bottom vessel ofa circular cross-section (Fig. 1a). The height (H) and diameter (D) of the vessel are equal ($H = D =$ 400 mm). The vessel has four baffles evenly distributed by 90°. The length of the baffle is (l) which is given by the ratio $l/D = 0.05$, 0.1, 0.15 and 0.25. The vessel is assumed to be completely filled with a complex shear-thinning fluid. The cylindrical vessel is equipped with a two-bladed impeller (Fig. 1b) or a four-bladed impeller (Fig. 1c). The diameter of the impeller

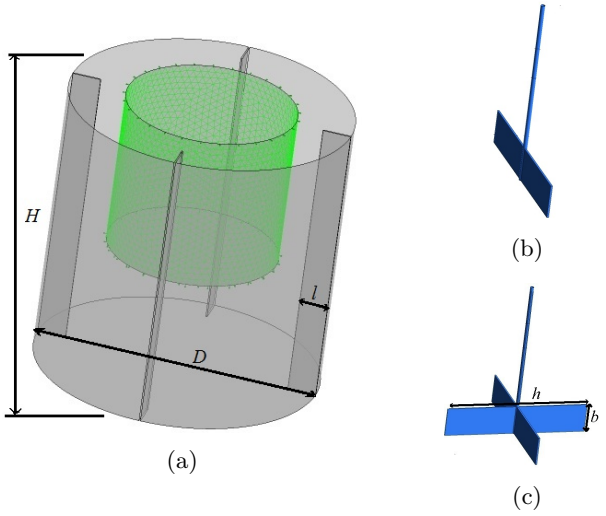

(a) (b) (c)

Figure 1: General view on the mixing system.

is equal to $h = D/2$, while the height of the impeller blade (b) is given by the ratio $b/D = 0.1$. The agitator is placed in the vessel at the clearance $D/2$. The thickness of the blade is 2 mm. The impeller rotates at a uniform speed expressed in terms of Reynolds number.

3 Mathematical formulation

The fluid used in this research is of polymer type, which has the behaviour of a shear-thinning fluid. For the shear-thinning fluids, the dynamic viscosity (μ) becomes apparent and it is expressed according to the Oswald model as:

$$\mu = m\dot{\gamma}^{n-1}, \tag{1}$$

where $\dot{\gamma}$ is the shear rateThis type of apparent dynamic viscosity is specific to shear-thinning fluids, meaning that as the shear rate between fluid layers increases, this dynamic viscosity decreases. This type of fluid has two rheological characteristics, namely, the flow consistency (m), and the power-law index (n), which are evaluated as 13.2×10^{-3} Pa s^n and 0.85×10^{-3} Pa s^n, respectively. The density of this fluid is 998 kg/m^3. These values were taken from the results of experimental work done by Venneker *et al.* [31].

In order to control the flow regime, the rotation of the impeller is expressed by the Reynolds number:

$$\mathrm{Re} = \frac{\rho N^{2-n} D^2}{m k_s^{n-1}}, \tag{2}$$

where ρ and N refer to the fluid density and rotational speed of the impeller. k_s is the weak function, it is a dimensionless value which is equal to 11.5. This value is taken from [20].

The power consumption is characterized by a dimensionless quantity which is called the power number as:

$$N_p = \frac{P}{\rho N^3 D^5}, \tag{3}$$

where P is the power consumption and it is calculated as:

$$P = \mu \int\limits_{\text{vessel volume}} Q_v \, dv, \tag{4}$$

where dv is written in cylindrical coordinates as:

$$dv = r \, dr \, d\theta \, dz, \tag{5}$$

Q_v indicates the viscous dissipation:

$$Q_v = \frac{1}{\mu^2}\left(2\tau_{rr}^2 + 2\tau_{\theta\theta}^2 + 2\tau_{zz}^2 + 2\tau_{rz}^2 + 2\tau_{r\theta}^2 + 2\tau_{z\theta}^2\right), \tag{6}$$

where

$$\tau_{rr} = -2\mu\left(\frac{\partial v_r}{\partial r}\right), \tag{7}$$

$$\tau_{r\theta} = -\mu\left[r\frac{\partial\left(\frac{v_\theta}{r}\right)}{\partial r} + \frac{1}{r}\frac{\partial v_r}{\partial \theta}\right], \tag{8}$$

$$\tau_{rz} = -\mu\left(\frac{\partial v_r}{\partial z} + \frac{\partial v_z}{\partial r}\right). \tag{9}$$

Equations (1)–(9) can be used to solve differential equations that model the fluid behaviour. These equations can be written as follows [45–47]:

$$\frac{1}{r}\frac{\partial(\rho r V_r)}{\partial r} + \frac{1}{r}\frac{\partial(\rho r V_\theta)}{\partial \theta} + \frac{\partial(\rho r V_z)}{\partial z} = 0, \tag{10}$$

$$\rho\left(V_r\frac{\partial V_r}{\partial r} + \frac{V_\theta}{r}\frac{\partial V_r}{\partial \theta} + V_z\frac{\partial V_r}{\partial z} - \frac{V_\theta^2}{r}\right) = -\frac{\partial p}{\partial r} + \mu\left[\frac{\partial}{\partial r}\left(\frac{1}{r}\frac{\partial}{\partial r}(rV_r)\right) + \frac{1}{r^2}\frac{\partial^2 V_r}{\partial \theta^2} + \frac{\partial^2 V_r}{\partial z^2} - \frac{2}{r^2}\frac{\partial V_\theta}{\partial \theta}\right], \tag{11}$$

$$\rho\left(V_r\frac{\partial V_\theta}{\partial r} + \frac{V_\theta}{r}\frac{\partial V_\theta}{\partial \theta} + V_z\frac{\partial V_\theta}{\partial z} + \frac{V_r V_\theta}{r}\right) = -\frac{1}{r}\frac{\partial p}{\partial \theta} + \mu\left[\frac{\partial}{\partial r}\left(\frac{1}{r}\frac{\partial}{\partial r}(rV_\theta)\right) + \frac{1}{r^2}\frac{\partial^2 V_\theta}{\partial \theta^2} + \frac{\partial^2 V_\theta}{\partial z^2} + \frac{2}{r^2}\frac{\partial V_r}{\partial \theta}\right], \tag{12}$$

$$\rho\left(V_r\frac{\partial V_z}{\partial r} + \frac{V_\theta}{r}\frac{\partial V_z}{\partial \theta} + V_z\frac{\partial V_z}{\partial z}\right) = -\frac{\partial p}{\partial z} + \mu\left[\frac{1}{r}\frac{\partial}{\partial r}\left(r\frac{\partial V_z}{\partial r}\right) + \frac{1}{r^2}\frac{\partial^2 V_z}{\partial \theta^2} + \frac{\partial^2 V_z}{\partial z^2}\right]. \tag{13}$$

These equations are written in dimensional form, some non-dimensional variables are given as:

$$(r^*, Z^*) = \frac{(r,z)}{D}, \qquad (V_r^*, V_\theta^*, V_z^*) = \frac{(V_r, V_\theta, V_z)}{ND}, \qquad p^* = \frac{p}{\rho(ND)^2}, \qquad R^* = \frac{2r}{D}. \tag{14}$$

4 Simulation steps

Since the vessel includes baffles, multiple reference frame (MRF) technique was employed. This technique mainly depends on dividing the domain of computation into two main parts. The first part is fixed and includes the walls of the vessel with the baffles, while the second is in rotation and includes the impeller. This technique was used in many previous works, including [2, 18, 19]. In the absence of baffles inside the vessel, a rotating reference frame (RRF) can be used as in works [1, 3, 8].

In order to achieve this simulation, both static and movable parts were created by using Gambit. A tetrahedral mesh with concentration of elements around the impeller was generated as it is shown in Fig. 2. The grid elements are constructed in this way because the flow layers are very sensitive in the vicinity of the impeller, which is the main cause of the fluid motion. The number of grid elements was selected based on the results of grid independency tests.

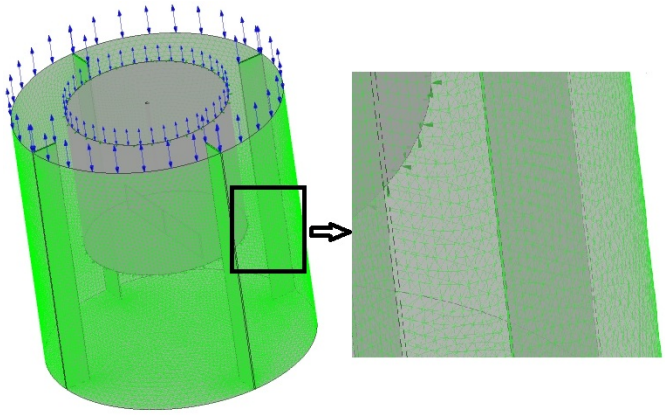

Figure 2: Computational mesh of the mixing domain.

The commercial computational fluid dynamics package Ansys-CFX was used to perform the calculations, solving the differential equations of conservation of mass and momentum (continuity and Navier-Stokes equations). The SIMPLE (semi-implicit method for pressure linked equations) algorithm was used for pressure-velocity coupling. The calculation results terminate when the residua in equations become less than 10^{-7}. No-slip boundary condition was employed around the walls of the impeller and the vessel. This condition provides the velocity gradient due to the effect of viscosity.

5 Results and discussion

Before presenting the new results we must verify the effectiveness of the method used in solving the considered problems. Therefore, we repeated the same experiment that was done by Youcefi *et al.* [32] and Ameur and Bouzit [8]. The first work is experimental, while the second work is numerical. Both works concentrate on a two-bladed impeller that rotates at a certain speed in a cylindrical vessel. The comparison of results between previous works and our results is shown in Fig. 3. The first graph shows the change of tangential velocity along the radius of the vessel. The graph shows a good agreement between the results. The second graph is for the variation of power number as a function of Reynolds number. Also, this graph shows a good agreement between the results.

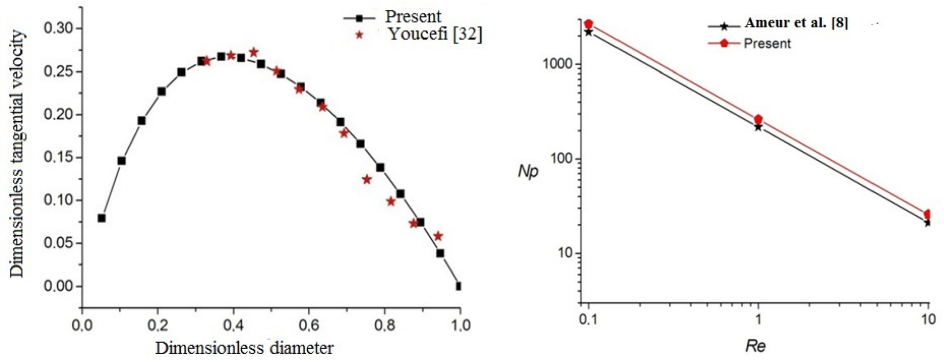

Figure 3: Validation test.

Figure 4 shows the effect of rotational speed and the number of blades on the fluid motion in the middle section of the vessel with respect to the direction z ($Z^* = z/D = 0.5$), for the vessel without baffles. Note that there are steady vortices near the walls of the container in the first case (two-bladed impeller), for Re = 50. But as the fluid speed increases, either by increasing the rotational speed or increasing the number of blades, this gradually dampens these vortices. This observation is similar to the one that was made in the previous work [2]. In other words, when the movement of the impeller is weak, vortices form near the impeller, while they disappear when the mixing speed increases. Furthermore, it is deduced from Fig. 4 that increasing the number of blades accelerates the movement of the fluid inside the vessel.

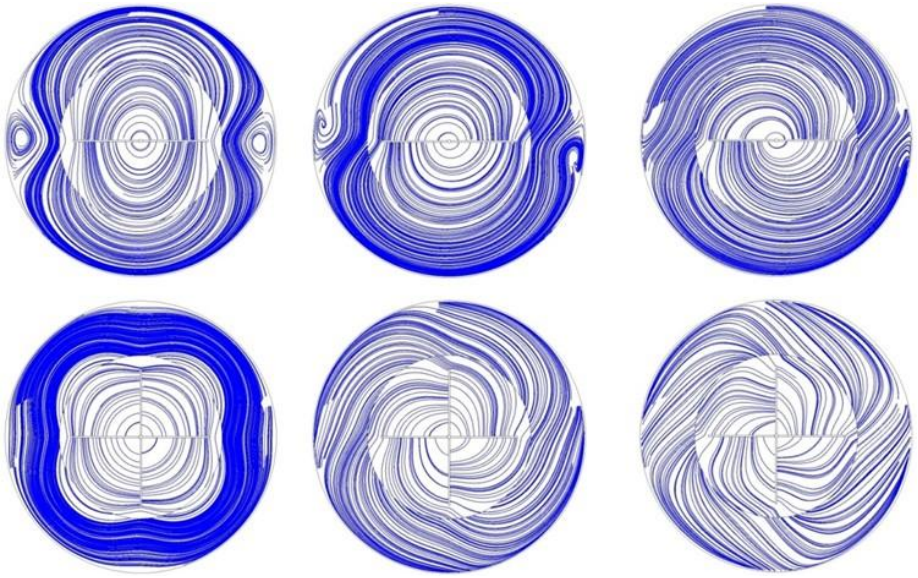

Re = 50 Re = 100 Re = 1000

Figure 4: Streamlines at $Z^* = 0.5$ and $l/D = 0$ for three values of Re; two-bladed impeller (top), four-bladed impeller (bottom).

Figure 5 presents the tangential velocity contours as a function of Reynolds number and the number of blades. Note that the greater the Reynolds num-

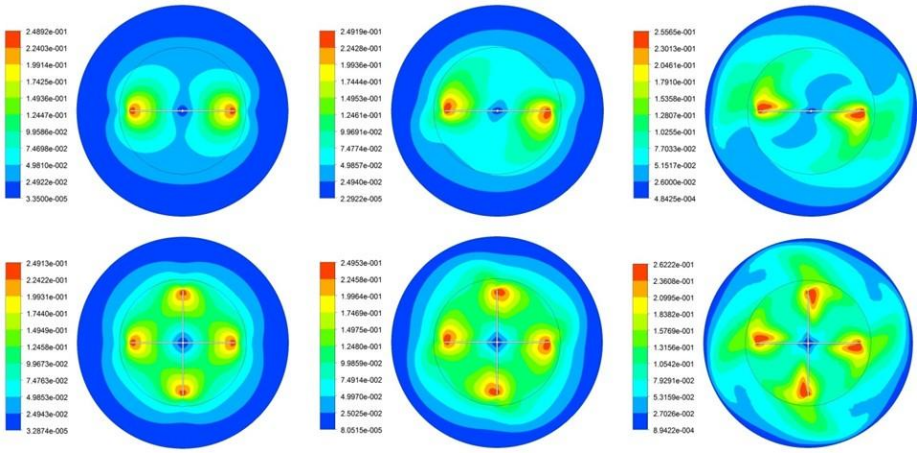

Re = 50 Re = 100 Re = 1000

Figure 5: Contours of tangential velocity at $Z^* = 0.5$ and $l/D = 0$ four three values of Re; two-bladed impeller (top), four-bladed impeller (bottom).

ber and/or the number of blades, the greater the fluid velocity expansion within the space, which gives the mixing efficiency.In addition to this, the uniform distribution of velocity indicates that the studied physical phenomenon has no evolution in terms of time. It is also noted that the fluid velocity is at its maximum value near the blades of the impeller and then gradually decreases towards the wall of the vessel. Figure 6 illustrates the linear distribution of the tangential velocity along the container radius. Values of the velocity and the location are written non-dimensionally. These values are taken at three locations in the direction Z^*, 0.25, 0.5 and 0.75, at a fixed value of Re = 50. It is noticed that the fluid speed increases closer to the impeller location. Also, the greater the number of blades, the higher the fluid velocity.

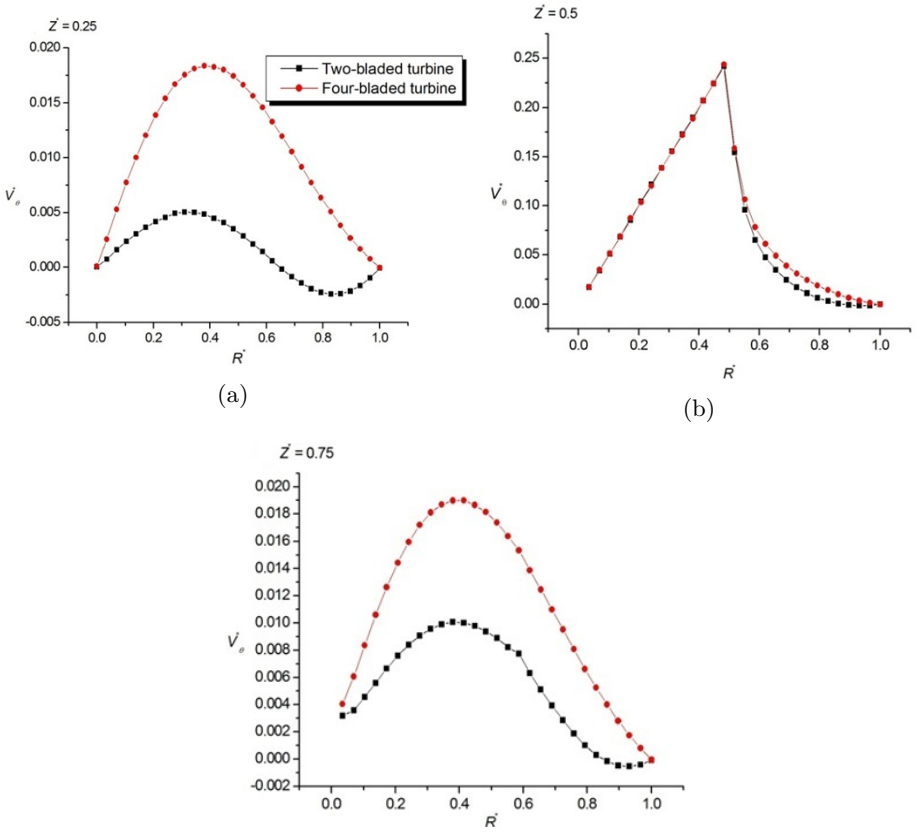

Figure 6: Dimesnionless tangential velocity (V_θ^*) along the diemensionless radius (R^*) of the vessel for Re = 50: (a) $Z^* = 0.25$, (b) $Z^* = 0.5$, (c) $Z^* = 0.75$.

Figure 7 shows the streamlines at the height $Z^* = 0.5$ of the vessel for three values of baffle length ratio (l/D) and for the rotational speed corresponding to Re = 100. The first row is for the case of a two-bladed impeller and the second row is for the case of a four-bladed impeller. It is clear that there is a formation of recirculation zones around the baffles. The size of these zones increases gradually with the increasing length of the baffles.

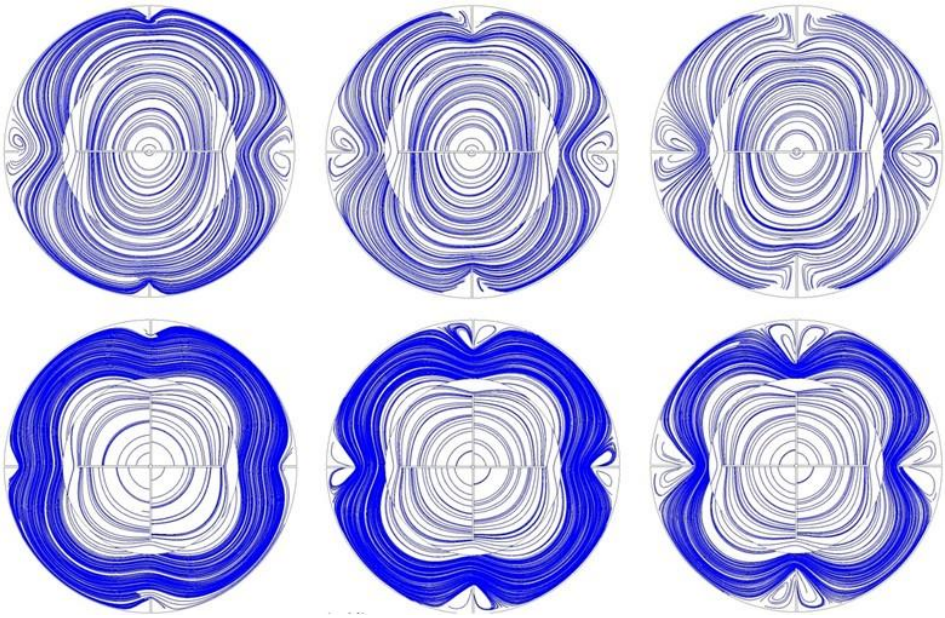

Figure 7: Streamlines at $Z^* = 0.5$ and Re = 100 for three values of the ratio l/D; two-bladed impeller (top), four-bladed impeller (bottom).

Figure 8 shows the tangential velocity contours at the same height ($Z^* = 0.5$) and under the same previous conditions. It is noted that the increase in the length of baffles reduces the flow velocity.

Figure 9 shows the distribution of tangential velocity along the radius of the vessel at the height of $Z^* = 0.25$ of the vessel for three baffle length ratios for the case of a two-bladed impeller and the case of a four-bladed impeller. The rotational speed of the impeller is constant in all cases and corresponds to the value of Reynolds number equal to 500. It is noticed that as the length of the baffles increases, the value of the flow velocity

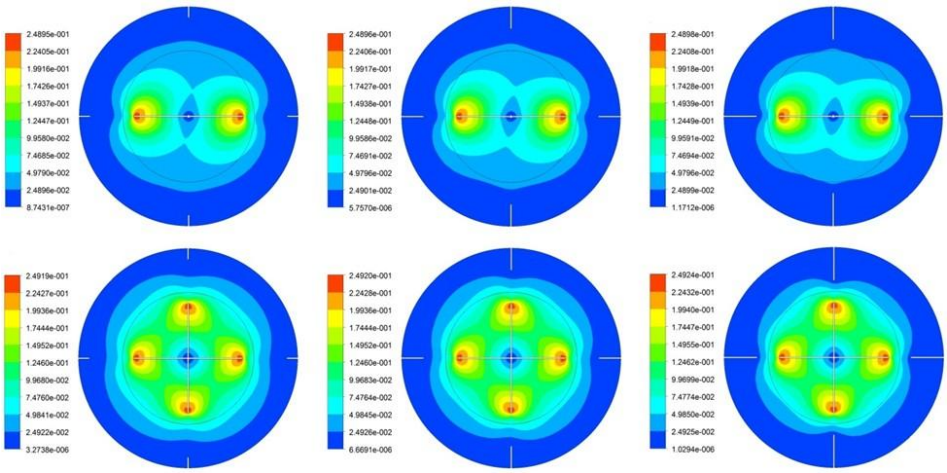

$l/D = 0.05$ $l/D = 0.1$ $l/D = 0.15$

Figure 8: Contours of tangential velocity at $Z^* = 0.5$ and $l/D = 0$ four three values of Re; two-bladed impeller (top), four-bladed impeller (bottom).

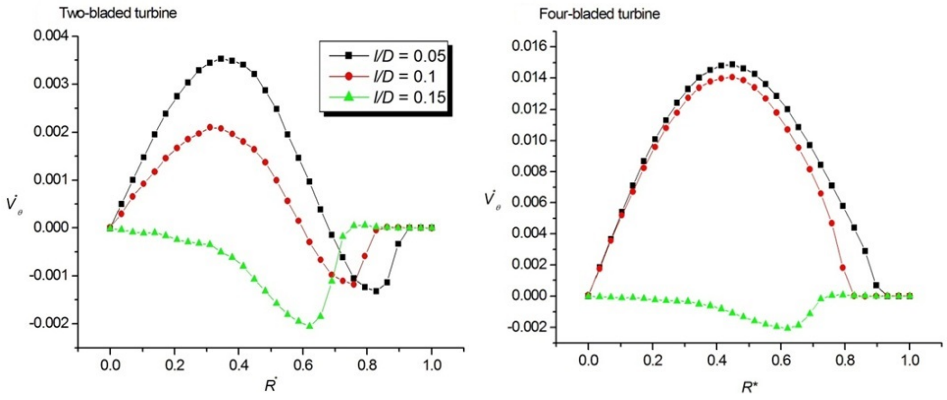

(a) (b)

Figure 9: Dimensionless tangential velocity (V_θ^*) along the dimensionless radius (R^*) of the vessel for $Z^* = 0.25$ and different ratios of l/D at Re = 500: (a) two-bladed impeller, (b) four-bladed impeller.

decreases. The baffle makes the value of the velocity zero next to it and this is very evident at the end of the graphs of the first and second case. It is also noticed that the presence of the baffle has the ability to change the pattern of fluid motion inside the container.

Figure 10 shows the variation of the power number versus Reynolds number and the baffle length ratio. The first graph (Fig. 10a) is for the case of a two-bladed agitator and the graph (Fig. 10b) is for the case of a four-bladed agitator. Before proceeding with analyses of the figure, we remember that the shear-thinning fluid in the one that the increased flow velocity decreases the viscosity of the fluid. Then, it is clear that the increase inthe number of blades increases the power number due to the increase of fluid friction. On the other hand, for the two cases considered, an increase in the value of Re decreases the value of power number due to the decrease of the fluid viscosity with the increasing flowvelocity. However, the effect of length of the baffles is clearly absent for both casesof two-bladed and four-bladed impellers. The power number decreases with Re, because with the increase of Re, the frictional force is reduced, and this is what reduces the total energy of the impeller.

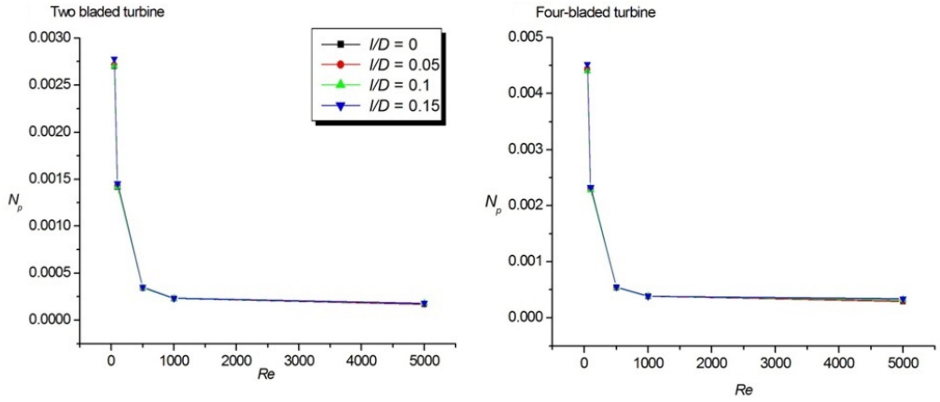

(a) (b)

Figure 10: Variation of power number versus Re and ratio l/D: (a) two-bladed impeller, (b) four-bladed impeller.

6 Conclusions

This work describes the results of numerical simulation of a complex fluid in a mechanical mixer. The work was carried out in order to understand the mixing process of this fluid. Some geometrical modifications were performed in order to know their effect on the mixing process. The points dealt with are: the rotational speed of the impeller, the number of blades and the length of the baffles added on the vessel wall. The effect of these parameters

on the flow velocity in the vessel and the consumed mechanical energy was investigated. After analyzing the results, the following facts were noted:

- Increasing the number of blades and/or the rotational speed of the impeller increases the flow velocity inside the vessel.
- The presence of the baffles on the vessel walls obstructs the flow motion, and this is what makes the speed of the flow decrease as the length of the baffles increases.
- The power number decreases as the rotational speed increases, while the length of the baffles has no effect on this number.
- The power number increases with the increasing number of blades.
- As for the fluid motion, it is more consistent with the higher rotational speed of the impeller.

Received 13 February 2023

References

[1] Hadjeb A., Bouzit M., KamlaY., Ameur H.: *A new geometrical model for mixing of highly viscous fluids by combiningtwo-blade and helical screw agitators*. Pol. J. Chem. Technol. **19**(2017), 3, 83–9l.

[2] Laidoudi H.: *Hydrodynamic analyses of the flow patterns in stirred vessel of two-bladed impeller*. J. Serb. Soc. Comput. Mech. **14**(2020), 2, 117–132.

[3] Ameur H.: *Agitation of yield stress fluids in different vessel shapes*. Eng. Sci. Technol. Int. J. **19**(2016), 1, 189–196.

[4] Galindo E., Nienow A.W.: *Mixing of highly viscoussimulated xanthan fermentation broths with the Lightnin A-315 impeller*. Biotechnol. Prog. **8**(1992), 3, 233–239.

[5] Galindo E., Nienow A.W.: *Performance of the Scaba 6SRGT agitator in mixing of simulated xanthan gumbroths*. Chem. Eng. Technol. **16**(1993), 2, 102–108.

[6] Amanullah A., Hjorth S.A., Nienow A.W.: *Cavern sizes generated in highly shear thinning viscous fluids by Scaba 3SHP1 impellers*. Food Bioprod. Process. **75**(1997), 4, 232–238.

[7] Pakzad L., Ein-Mozaffari F., Chan P.: *Using computational fluid dynamics modeling to study the mixing of pseudoplastic fluids with a Scaba 6SRGT impeller*. Chem. Eng. Process. **47**(2008), 12, 2218–2227.

[8] Ameur H., Bouzit M.: *Power consumption for stirring shear thinning fluids by two-blade impeller*. Energy **50**(2013), 326–332.

[9] Ameur H., Bouzit M., Ghenaim A.: *Numerical studyof the performance of multistage Scaba 6SRGT impellersfor the agitation of yield stress fluids in cylindrical tanks.* J. Hydrodyn. **27**(2015), 3, 436–442.

[10] Patel D., Ein-Mozaffari F., Mehrvar M.: *Improvingthe dynamic performance of continuous-flow mixing ofpseudoplastic fluids possessing yield stress using Maxblend impeller.* Chem. Eng. Res. Des. **90**(2012), 4, 514–523.

[11] Kazemzadeh A., Ein-Mozaffari F., Lohi A.: *Investigation of hydrodynamic performances of coaxial mixersin agitation of yield-pseudoplasitc fluids: single and double-central impellers in combination with the anchor.* Chem. Eng. J. **294**(2016), 417–430.

[12] Kazemzadeh A., Ein-Mozaffari F., Lohi A.: *Effect of the rheological properties on the mixing of Herschel-Bulkley fluids with coaxial mixers: applications of tomography, CFD, and response surface methodology.* Can. J. Chem. Eng. **94**(2016), 12, 2394–2406.

[13] Ammar M., Abid M.S.: *Numerical investigation of turbulent flow generated in baffled stirred vessels equipped with three different turbines in one and two-stage system.* Energy **36**(2011), 8, 5081–5093.

[14] Vilard G., Verdone N.: *Production of metallic iron nanoparticles in a baffled stirred tank reactor: Optimization via computational fluid dynamics simulation.* Particuology **52**(2020), 83–96.

[15] Laidoudi H., Ameur H.: *Complex fluid flow in annular space under the effects of mixed convection and rotating wall of the outer enclosure.* Heat Transfer **51**(2022), 5, 3741–3767.

[16] Tacay C.D., Payunescu M.: *Suspension of solid particles in spherical stirred vessels.* Chem. Eng. Sci. **55**(2000), 15, 2989–2993.

[17] Vakili M.H., Esfahany M.N.: *CFD analysis of turbulence in a baffled stirred tank, a three-compartment model.* Che. Eng. Sci. **64**(2009), 2, 351–362.

[18] Foukrach M., Bouzit M., Ameur M., Kamla Y.: *Influence of the vessel shape on the performance of a mechanically agitated system.* Chem. Pap. **73**(2019), 469–480.

[19] Laidoudi H., Ameur H.: *Investigation of the mixed convection of power-law fluids between two horizontal concentric cylinders: Effect of various operating conditions.* Therm. Sci. Eng. Prog. **20**(2020), 100731.

[20] Ameur H.: *Mixing of shear thinning fluids in cylindrical tanks: Effect of the impeller blade designand operating conditions.* Int. J. Chem. React. Eng. **14**(2016), 1025–1033.

[21] Ghotli R.A., Abdul Aziz A.R., Ibrahim S., Baroutian S., Niya A.A.: *Study of various curved-blade impeller geometrieson power consumption in stirred vessel using response surface methodology.* J. Taiwan Inst. Chem. Eng. **44**(2013), 2, 192–201.

[22] Khapre A., Munshi B.: *Numerical investigation of hydrodynamic behavior of shear thinning fluids in stirred tank.* J. Taiwan Inst. Chem. Eng. **56** (2015), 16–27.

[23] Luan D., Chen Q., Zhou S.: *Numerical simulation and analysis of power consumption and Metzner-Otto constant for impeller of 6PBT.* Chin. J. Mech. Eng. **27**(2014) 635–640.

[24] Sossa-Echeverria J., Taghipour F.: *Computational simulation of mixing flow of shear thinning non-Newtonianfluids with various impellers in a stirred tank*. Chem. Eng. Proc. **93**(2015), 66–78.

[25] Woziwodzki S., Broniarz-Press L., Ochowiak M.: *Transitional mixing of shear-thinning fluids in vessels with multiple impellers*. Chem. Eng. Techn. **33**(2010), 7, 1099–1106.

[26] Zhao J., Gao Z., Bao Y.: *Effects of the blade shape on the trailing vortices in liquid flow*. Chin. J. Chem. Eng. **19**(2011), 2, 232–242.

[27] Khopkar A.R., Mavros P., Ranade V.V., Bertrand J.: *Simulation of flow generated by an axial-flow impeller: batch and continuousoperation*. Chem. Eng. Res. Des. **82**(2004), 6, 737–751.

[28] Konfršt B., Konfršt J., Fořt I., Kotek M., Chára Z. *Study of the turbulent flow structure around astandard Rushton impeller*. Chem. Process. Eng. **35**(2014), 1, 137–147.

[29] Hartmann H., Derksen J.J., Montavon C., Pearson J., Hamill I.S.: *Assessment of large eddy and RANS stirredsimulations by means of LDA*. Chem. Eng. Sci. **59**(2004), 2419–2432.

[30] Devarajulu C., Loganathan M.: *Effect of impeller clearance and liquid level on critical impeller speed in an agitated vesselusing different axial and radial impellers*. J. Appl. Mech. **9**(2016), 6, 2753–2761.

[31] Venneker B., Derksen J., Vanden Akker H.E.A.: *Turbulent flow of shear-thinning liquids in stirred tanks – The effects of Reynolds number and flow index*. Chem. Eng. Res. Des. **88**(2010), 7, 827–43.

[32] Youcefi A.: *Etude expérimentale de l'écoulement de fluide viscoélastique autour d'un agitateur bipale dans une cuve agitée*. (*Experimental study of viscoelastic fluid flow around two-blade impeller in a stirred vessel*). PhD thesis, Ecole Nationale Polytechnique, Toulouse 1993 (in French).

[33] Ahmed S., Mansour M., Hussein A.K., Sivasankaran S.: *Mixed convection from a discrete heat source in enclosures with two adjacent moving walls and filled with micropolar nanofluids*. Eng. Sci. Tech. Int. J. **19**(2016), 1, 364–376.

[34] Laidoudi H., Helmaoui M.: *Enhancement of natural convection heat transfer in concentric annular space using inclined elliptical cylinder*. J. Naval Archit. Mar. Eng. **17**(2020), 2, 89–99.

[35] Al-Rashed A., Aich W., Kolsi L., Mahian O., Hussein A.K., Borjini M.: *Effects of movable-baffle on heat transfer and entropy generation in a cavity saturated by CNT suspensions: Three-dimensional modeling*. Entropy **19**(2017), 5, 200–216.

[36] Laidoudi H., Bouzit M.: *The effect of asymmetrically confined circular cylinder and opposing buoyancy on fluid flow and heat transfer*. Defect Diffus. Forum **374**(2017), 18–28.

[37] Hussein A.K., Rout S., Fathinia F., Chand R., Mohammed H.: *Natural convection in a triangular top wall enclosure with a solid strip*. J. Eng. Sci. Tech. **10**(2015), 10, 1326–1341.

[38] Acharya N.: *Buoyancy driven magnetohydrodynamic hybrid nanofluid flow within a circular enclosure fitted with fins*. Int. Commun. Heat Mass Transf. **133**(2022), 105980.

[39] Li Z., Hussein A.K., Younis O., Afrand M., Feng S.: *Natural convection and entropy generation of a nanofluid around a circular baffle inside an inclined square cavity under thermal radiation and magnetic field effects*. Int. Commun. Heat Mass Transf. **116**(2020), 104650.

[40] Acharya N., Maity S., Kundu P.K.: *Differential transformed approach of unsteady chemically reactive nanofluid flow over a bidirectional stretched surface in presence of magnetic field*. Heat Transf. **49**(2020), 6, 3917–3942.

[41] Hassouni S., Laidoudi H., Makined O.D., Bouzit M., Haddou B.: *A qualitative study of mixing a fluid inside a mechanical mixer with the effect of thermal buoyancy*. Arch. Thermodyn. **44**(2023), 1, 105–119.

[42] Bulat P.V., Volkov K. N.: *Fluid/solid coupled heat transfer analysis of a free rotating disc*. Arch. Thermodyn. **39**(2018), 3, 169–192.

[43] Bouakkaz R., Ouali A.E., Khelili Y., Faouzi S., Tiauiria I.: *Unconfined laminar nanofluid flow and heat transfer around a rotating circular cylinder dissipating uniform heat flux in the steady regime*. Arch. Thermodyn. **40**(2019), 4, 3–20.

[44] Bouakkaz R., Salhi F., Khelili Y., Quazzazi M., Talbi K.: *Unconfined laminar nanofluid flow and heat transfer around a rotating circular cylinder in the steady regime*. Arch. Thermodyn. **38**(2017), 2, 3–20.

[45] Ramla M., Laidoudi H., Bouzit M.: *Behaviour of a non-newtonian fluid in a helical tube under the influence of thermal buoyancy*. Acta Mech. Autom. **16**(2022), 2, 111–118.

[46] Mokeddem M., Laidoudi H., Makinde O.D., Bouzit M.: *3D simulation of incompressible poiseuille flow through 180 curved duct of square cross-section under effect of thermal buoyancy*. Period. Polytech. Mech. Eng. **63**(2019), 4, 257–269

[47] Mokeddem M., Laidoudi H., Bouzit M.: *3D simulation of Dean vortices at 30 position of 180 curved duct of square cross-section under opposing buoyancy*. Defect Diffus. Forum **389**(2018), 153–163.